How frequency hopping suppresses pulse-echo ambiguity in bat biosonar

Chen Ming[a], Mary E. Bates[b], and James A. Simmons[a,1]

[a]Department of Neuroscience, Carney Institute, Brown University, Providence, RI 02912; and [b]Private address, Arlington, MA 02474

Edited by Terrence J. Sejnowski, Salk Institute for Biological Studies, La Jolla, CA, and approved May 31, 2020 (received for review January 19, 2020)

Big brown bats transmit wideband FM biosonar sounds that sweep from 55 to 25 kHz (first harmonic, FM1) and from 110 to 50 kHz (second harmonic, FM2). FM1 is required to perceive echo delay for target ranging; FM2 contributes only if corresponding FM1 frequencies are present. We show that echoes need only the lowest FM1 broadcast frequencies of 25 to 30 kHz for delay perception. If these frequencies are removed, no delay is perceived. Bats begin echo processing at the lowest frequencies and accumulate perceptual acuity over successively higher frequencies, but they cannot proceed without the low-frequency starting point in their broadcasts. This reveals a solution to pulse-echo ambiguity, a serious problem for radar or sonar. In dense, extended biosonar scenes, bats have to emit sounds rapidly to avoid collisions with near objects. But if a new broadcast is emitted when echoes of the previous broadcast still are arriving, echoes from both broadcasts intermingle, creating ambiguity about which echo corresponds to which broadcast. Frequency hopping by several kilohertz from one broadcast to the next can segregate overlapping narrowband echo streams, but wideband FM echoes ordinarily do not segregate because their spectra still overlap. By starting echo processing at the lowest frequencies in frequency-hopped broadcasts, echoes of the higher hopped broadcast are prevented from being accepted by lower hopped broadcasts, and ambiguity is avoided. The bat-inspired spectrogram correlation and transformation (SCAT) model also begins at the lowest frequencies; echoes that lack them are eliminated from processing of delay and no longer cause ambiguity.

echolocation | bat biosonar | echo ambiguity | clutter suppression | sonar image

Big brown bats (*Eptesicus fuscus*) (1) use echolocation to sense their surroundings by broadcasting trains of ultrasonic sounds and listening for echoes that return to their ears (2–4). They are insectivorous and feed primarily on beetles and moths (5). Prey are captured in open flight and from vegetation or the ground in cluttered spaces (6). Big brown bats' biosonar broadcasts are brief, frequency-modulated (FM) sounds ("chirps"), covering about 25 to 110 kHz in two prominent harmonic sweeps (first harmonic [FM1] and second harmonic [FM2]; Fig. 1*A*) (8, 9). Big brown bats fly and orient effectively in real time through sonar scenes that go from simple, such as chasing a single flying insect in the open, to complex, such as hunting in spaces surrounded by vegetation, taking prey off the ground, or flying along corridors through vegetation (6, 10, 11). Complex, highly cluttered conditions such as those that bats face routinely in their natural environment pose significant challenges for man-made systems (12), leading to consideration of whether biologically inspired sonar or radar designs might mitigate these problems. Here, we address the complicated story about how big brown bats cope with one such challenge—overcoming pulse-echo or range ambiguity when flying in clutter—and show that modifications of an existing bioinspired model (13) offer an effective solution.

Bats determine target range from echo delay (14). The temporal sequence of returning echoes is the basis for perceiving objects that comprise the scene. The dynamics of echolocation depend on the length of the epoch (echo delay) for receiving all of the echoes from each individual broadcast in relation to the time between successive broadcasts (interpulse interval [IPI]). Echoes from the nearest objects arrive quickly, while echoes from objects located farther away arrive after longer delays (~6 ms per meter of target range). For example, the echo epoch could last up to about 60 ms for the farthest objects at long ranges up to 10 m but nevertheless contain numerous echoes from objects at shorter ranges (15). After a broadcast is sent out, the epoch begins immediately and extends for several tens of milliseconds until it encompasses the depth of the entire biosonar scene (10, 11). If the bat waits until all of the echoes of one transmitted pulse have arrived before emitting the next pulse (IPI > echo epoch), the streams of echoes that follow successive pulses remain separate—they do not intermingle (Fig. 2*A*) (17). In this condition, all of the objects in the scene are unambiguously and separately registered for both pulses. During pursuit of insects in open spaces, bats universally shorten their IPIs for rapid updates of target location to guide interception, but there are no echoes other than those of the target that return later and could cause ambiguity. In cluttered conditions, however, the nearest objects can pose collision hazards, and bats shorten their IPIs to react in time to avoid hitting anything. Other objects farther away nevertheless return more echoes at longer delays, which can extend the echo epoch beyond the IPI itself (17). When two successive broadcasts are emitted so close together that the echo epoch for the first pulse still is in progress when the second pulse is emitted and its corresponding echo epoch begins (IPI < echo epoch), the two streams of echoes

Significance

The wide frequency spectrum of FM bat biosonar sounds enables accurate perception of echo delay (target distance) by contributing numerous delay estimates across frequencies. However, bats require the lowest frequencies in the broadcast to be present in echoes for all higher frequencies to contribute, too. By incorporating this feature into an existing auditory model of FM biosonar, the model can reject echoes that lack the lowest frequencies in the most recent broadcast, thus suppressing echoes of an earlier broadcast that has slightly higher low-end frequencies. This biologically inspired method adopts the bat's frequency-hopping technique to suppress pulse-echo ambiguity in wideband systems, a serious problem for man-made wideband radar and sonar systems.

Author contributions: M.E.B. and J.A.S. designed research; M.E.B. performed research; C.M. and J.A.S. analyzed data; J.A.S. wrote the paper; and C.M. developed the computational SCAT model.

The authors declare no competing interest.

This article is a PNAS Direct Submission.

Data deposition: All data and programs are available on GitHub, https://github.com/gomingchen/SCAT.

[1]To whom correspondence may be addressed. Email: james_simmons@brown.edu.

First published July 6, 2020.

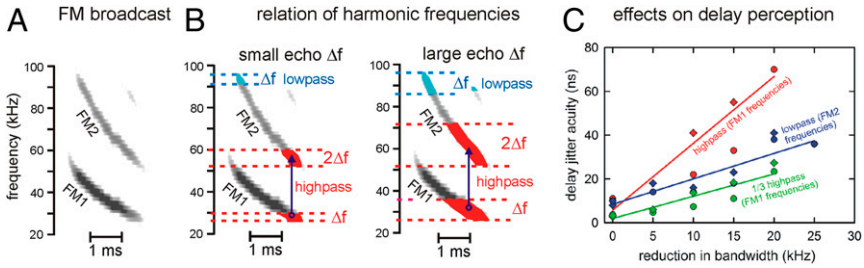

Fig. 1. Role of FM harmonics in echo delay perception. (*A*) FM broadcast spectrogram has two down-sweeping harmonics (FM1: 55 to 25 kHz, FM2: 100 to 50 kHz). (*B*) Expected effects of low-pass (blue symbols and text) and high-pass (red symbols and text) filtering of echo spectra on delay acuity. Slight low-pass filtering of echoes by a small Δf = 4 kHz (narrow blue area at top of FM2 sweep) truncates the upper end of the echo spectrum by only that amount. Stronger low-pass filtering by larger Δf = 10 kHz (wider blue area) still only affects the upper end of FM2. In contrast, slight high-pass filtering by a small Δf = 4 kHz (narrow red area at lower end of FM1 sweep) also removes the corresponding second harmonic by 2Δf = 8 kHz from FM2 (vertical blue arrow projecting to wider red segment at lower end of FM2), for a total frequency loss of 3Δf = 12 kHz. More extensive high-pass filtering by a large Δf = 14 kHz (broad red segment of FM1 sweep) also removes 2Δf = 28 kHz from FM2 (wider red segment of FM2), for a total frequency loss of 3Δf = 42 kHz. (*C*) Removal of lower FM1 frequencies reduces delay acuity 3 times more than removal of the same bandwidth in upper FM2 frequencies (replotted from ref. 7). Thresholds for delay acuity by two big brown bats detecting small changes in delay (vertical axis; circles and diamonds) in a series of echoes with different high-pass and low-pass cutoff frequencies expressed as reductions in frequency content (horizontal axis, Δf in kHz). Removing frequencies from the top of FM2 (115 dB/octave cutoffs from 89 down to 55 kHz) increases delay change detection thresholds from 10 to 36 ns (blue data points and regression line); removing frequencies from the bottom of FM1 (115 dB/octave cutoffs from 15 up to 35 kHz) increases thresholds from 10 to 71 ns (red data points and regression line). From spectrograms in *A*, the slope of the high-pass results should be 3 times steeper than the slope of the low-pass results because removal of FM1 frequencies is magnified by removal of corresponding FM2 frequencies. The high-pass data also are rescaled vertically by 1/3 (green data points and regression line), which now parallels the low-pass results.

intermingle (Fig. 2*B*) (16). Echoes of the first pulse then will arrive after the second pulse and thus are vulnerable to being registered as short-delay echoes from the second pulse rather than what they are—long-delay echoes from the first pulse (12, 16–18). The erroneously short delays of these echoes are likely to disrupt flight by inducing the bat to change its flight trajectory to avoid an imminent collision, even though the "true" objects are actually farther away. The nearer, ambiguous objects are phantoms.

The first solution for resolving ambiguity is for the bat to emit its broadcasts at alternating long and short IPIs, a common strategy in man-made systems (12). The short intervals provide rapid updates of the nearest objects for critical steering and collision avoidance, while the long intervals probe deeper into the scene as a whole to register the farthest objects in the background (17). This provides the bats some awareness of the whole scene and also the ability to react swiftly to potential collision hazards. Especially when flying in cluttered surroundings, big brown bats prominently emit broadcasts at alternating long and short IPIs, using interval sizes that depend on the density and proximity of the clutter (16, 19–26). However, the difficulty in the extreme is that when the IPIs are short enough, the streams of echoes from successive sounds frequently overlap to create ambiguity even though they are interspersed with long IPIs, often by alternating (Fig. 2*B*).

Frequency Hopping

A second solution for resolving pulse-echo ambiguity is to emit successive broadcasts at different frequencies by alternating them up and down to distinguish their corresponding echo streams from each other (13). This is "frequency hopping," a fundamental spread-spectrum technique (27) used by some species of bats that emit short, constant-frequency sounds (28, 29). To be effective, successive broadcasts that hop in frequency should hop far enough not to overlap in their spectra. Echoes of successive broadcasts then can be streamed as discriminable by their frequencies even though they overlap in the same echo epochs. In conditions of very short IPIs and pronounced ambiguity, big brown bats also have been shown to exhibit frequency hopping up (see the example in Fig. 2 *A* and *B*). High-fidelity recordings of successive FM broadcasts acquired by a radiotelemetry microphone ("telemike") carried by the flying bat show a frequency shift (Δf) up to about 5 to 7 kHz between the first broadcast and the second. Moreover, the size of frequency hopping (Δf in Fig. 2) depends quantitatively, and statistically significantly, on the amount of echo stream overlap or the degree to which echo epochs exceed IPIs (16). It disappears when the overlap of echo epochs, and the accompanying pulse-echo ambiguity, is gone. However, the big brown bat's broadcasts are wideband, covering 75 to 80 kHz (Fig. 1*A*), and therefore are still overlapping in their spectra by 70 to 80% despite the frequency hop (Fig. 2). They are not narrowband signals for which frequency hopping is technically feasible (12), and they are not the narrowband sounds used by echolocating bats that regularly exhibit frequency hopping (28, 29). To emphasize, when IPIs are short enough that successive echo epochs overlap, the bat alternates the beginning and ending frequencies in FM1 on successive broadcasts, upward in the first sound and downward in the second (Fig. 2*B* vs. Fig. 2*A*) (16). This automatically carries FM2 to correspondingly higher or lower frequencies due to FM2 2:1 harmonic relation, magnifying the disparity in the spectrograms between echoes in the two streams.

The use of frequency hopping by big brown bats using wideband biosonar sounds (Fig. 1*A*) raises the question of how such small frequency hops can lead to disambiguation of overlapping echo epochs when the majority of the echo spectra still overlap (Fig. 2). Through psychophysical experiments, we trace the bat's mechanism for solving this technologically critical problem, and we incorporate it into a computational solution for potential application to man-made systems. To get there, we have to consider how different frequencies contribute to perception of echo delays. In a conventional wideband radar or sonar system, a replica or template of the transmitted signal is stored in the receiver, and the incoming stream of echoes is cross correlated with this template to locate the instants in time when individual signals similar to the broadcast return (i.e., matched filtering; refs. 12 and 30). Overall delay accuracy is reciprocally related to echo bandwidth (30), and all of the frequencies in the original broadcast make equal contributions to the acuity for determining the delay. In contrast, experiments show that big brown bats treat the frequencies in its two harmonics (FM1, FM2) asymmetrically. First, on a coarse scale of delay, the presence of FM1 is necessary for echo delay to be perceived; echoes containing only

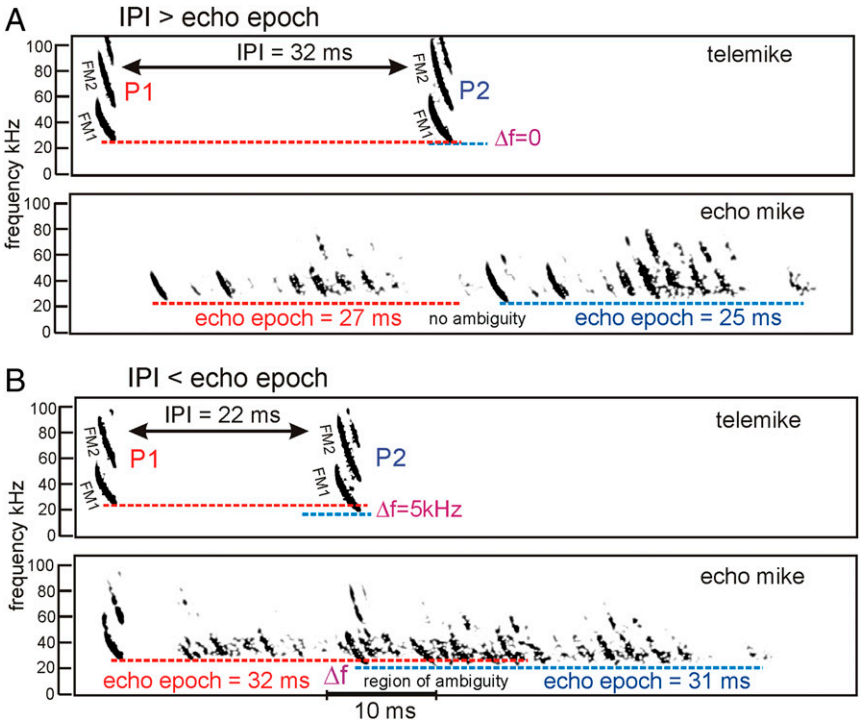

Fig. 2. Pulse-echo ambiguity and frequency hopping in FM bat sonar. Examples of spectrograms for successive big brown bat FM biosonar broadcast pulses (P1, P2) recorded by a miniature telemike attached to the flying bat (data replotted from ref. 16). A second echo microphone recorded echoes reflected back to the bat from multiple obstacles while the bat flew toward them. Each broadcast contains two prominent harmonic sweeps (FM1, FM2). (*A*) IPI of 32 ms is longer than the echo epoch of 27 ms, so all echoes of P1 are received before P2 is transmitted, and no ambiguity occurs. P1 ends at about the same frequency as P2 (Δf = 0; no frequency hopping). (*B*) IPI of 22 ms is shorter than the echo epoch of 32 ms, too short for all echoes of P1 to be received before P2 is transmitted. There is a region of ambiguity when lingering echoes of P1 are still arriving after P2 is emitted. These echoes could be registered ambiguously as echoes of P2 instead of P1, leading to perception of phantom obstacles at close range, which could disrupt orientation. The bat quantitatively and significantly responds to the occurrence of ambiguity by raising the ending frequency of P1 relative to P2 by the amount Δf, which is about 5 kHz (frequency hopping, ref. 16).

FM2 are not perceived as having a delay; indeed, they are not perceived as echoes at all (31–33). Second, on a fine scale of delay, the contributions of frequencies in FM1 and FM2 are quantitatively unequal. In a psychophysical task where echo delay alternates by different, very small increments from one broadcast to the next, big brown bats achieve very high acuity for detecting these minute, submicrosecond changes in echoes (34). In this task, as expected (30), selective removal of frequencies reduces echo bandwidth proportionally, and the bat's performance is degraded accordingly. Close to its threshold for detecting such small changes in delay, the bat exploits all of the frequencies contained in echoes to enhance its perceptual acuity (7). However, the asymmetry of the harmonics' contributions nevertheless is manifested by the perceptual effects of selective removal of segments from the echo spectrum in FM2 or FM1. For example, slight low-pass filtering truncates the upper end of the echo spectrum by a small amount (narrow blue area for Δf at the top of FM2 in Fig. 1*B*), and the bat's acuity declines slightly (Fig. 1*C*) (7). Stronger low-pass filtering causes further reduction in the echo spectrum (wider blue area for Δf at the top of FM2), and the loss in acuity is proportionally larger (Fig. 1*C*). Similarly, slight high-pass filtering truncates the lower end of FM1 by the same small amount (narrow red area for Δf at the lower end of FM1 in Fig. 1*B*). However, for purposes of perception, it not only removes that particular Δf segment of FM1, but it also removes the corresponding segment of 2Δf at the lower end of FM2. Because FM2 is the second harmonic, there are twice as many frequencies affected in FM2 as in FM1. The total span of frequencies prevented from contributing to delay change acuity in FM1 and FM2 together thus is 3 times the original deletion from FM1 (3Δf in Fig. 1*B*). More extensive high-pass filtering of FM1 (broad red area for Δf of the FM1 sweep in Fig. 1*B*) removes an even wider segment from FM2 (wider red area for 2Δf of FM2). The outsized effect of filtering FM1 occurs because the contribution of frequencies in FM2 is contingent upon the presence of corresponding FM1 frequencies. Removal of FM1 frequencies reduces effective echo bandwidth not merely by Δf but by 3Δf. The slopes of the regression lines in Fig. 1*C* show the performance of bats detecting small changes in echo delay (thresholds on the vertical axis) for echo stimuli with different high-pass and low-pass cutoff frequencies, expressed as the reduction in frequency content (Δf in Fig. 1*C*, horizontal axis) (7). Removing frequencies from the top of FM2 (low-pass cutoffs from 89 down to 55 kHz) increases delay change detection thresholds from 10 to 36 ns (blue data points and regression line). Removing frequencies from the bottom of FM1 (high-pass cutoffs from 15 up to 35 kHz) increases thresholds from 10 to 71 ns (red data points and regression line). To illustrate the asymmetric quantitative relation between frequencies in FM1 and FM2, the high-pass results are replotted in Fig. 1*C* as 1/3 of the actual high-pass threshold values (green data points and regression line). These now align in parallel with the low-pass results, demonstrating the 1:3 expectation derived from the spectrograms in Fig. 1*B*.

Experimental Design

Two factors converge on the design of experiments described here. First, the demonstrated primacy of FM1 over FM2 (Fig. 1 *B* and *C*) (7) suggests an even more restricted hypothesis than just the global asymmetry of the harmonics for perception: The hypothesis being tested here is that only the very lowest FM1 frequencies of 25 to 30

kHz are necessary for the bat to perceive delay. Their removal would prevent formation of a delay percept at all, a more radical limitation than the idea that the entire band of FM1 is necessary (31–33). Second, the small, seemingly not very effective, size of the frequency hopping by just a few kilohertz (most obviously as Δf at the tail end of FM1 in Fig. 2) suggests that the hypothesized necessity of these lowest FM1 frequencies may be the key to why the harmonics are processed asymmetrically. Using a two-alternative forced-choice behavioral paradigm (Fig. 3*A*), we carried out psychophysical experiments to test whether only the lowest frequencies in the bat's broadcasts are required for echoes to be perceived as having a well-defined delay. The procedure was to progressively filter out more and more frequencies at the lower end of the broadcast spectrum or the upper end of the broadcast spectrum to home in on any frequency region that might prove essential for perception of delay. The two-choice method has been proven to be effective for assessing echo delay acuity as well as the content of delay images perceived by bats (7, 14, 31–34, 36, 37). Here, four big brown bats (*Eptesicus fuscus*) were trained with food reward to sit on a Y-shaped platform (Fig. 3*A*) and broadcast sonar sounds into microphones (m, left and right) which lead to the return of electronic "virtual reality" echoes from loudspeakers (s, also left and right) (7, 14, 31–34, 36). Each of the bat's broadcasts gives rise to a simulated echo from the microphone–loudspeaker combination on the left and another from the loudspeaker–microphone combination on the right. Echo delay is determined electronically by adjustable delay lines, and echo frequency content is manipulated by low-pass or high-pass electronic filters (115 dB/octave roll-off specified at low-pass or high-pass −3 dB filter skirts; Fig. 3*A*). The bat's correct response is to move forward toward whichever loudspeaker delivers S+ echoes to receive its reward (a mealworm). The rewarded S+ echoes simulate a virtual object containing two reflecting parts (36, 38). They contain two closely spaced reflections, called acoustic highlights or glints (39), one reflection at a delay of 3,160 μs simulating a reflection from a distance of 54 cm and the other reflection at a slightly longer delay of 3,460 μs simulating a second reflection at a distance of 60 cm (Fig. 3*A*, S+ is blue). The actual experimental manipulations consist of low-pass or high-pass filtering of the S+ echoes at one of the low-pass cutoff frequencies (blue list in Fig. 3*A*) or high-pass cutoff frequencies (red list in Fig. 3*A*). The horizontal positions of the data points in Fig. 3*B* show these high-pass and low-pass filter cutoff frequencies superimposed on a representative spectrogram for a bat FM sound, displayed rotated sideways to have a horizontal frequency axis matching the performance plot. The other loudspeaker (Fig. 3*A*) delivers S− echoes (unrewarded; shown in purple). The S− echoes contain a single reflection at a longer delay of 3,660 μs simulating a one-glint target at a longer distance of 63 cm. No low-pass or high-pass filtering was imposed on S− echoes, which contained frequencies across the broadcast spectrum, just with slight losses above 85 kHz due to the loudspeakers' response. The delay difference of 500 μs between S+ and S− (simulated distance difference of over 8 cm) is easily discriminated by big brown bats (14). Moreover, the presence of two virtual glints in S+ simulated by the two reflections 300 μs apart also is easily perceived as an object with a distinctive three-reflector shape (38). Left–right positions of S+ and S− were randomized, and experimental conditions were tested for 150 trials by each of four big brown bats, whose performance was assessed as the percentage of correct responses (0% perfect; 50% chance, 25% threshold). Whichever way it is defined, the task is easy for bats—either discrimination of a 500 μs overall delay difference between S+ and S−, which is 10 times larger than the big brown bat's delay discrimination threshold of about 50 μs in this type of two-choice test (14), or of two-glint echoes with a 300 μs delay separation versus one-glint echoes at a longer overall delay. This glint spacing is well within the range of delay separations perceived by big brown bats as returning from an insect-sized two-glint target (38). The question is whether this easy task still is easy if the lowest frequencies in FM1 are removed from the S+ echoes.

The experimental protocol was approved by the Brown University Institutional Animal Care and Use Committee in keeping with NIH guidelines for animal research.

Results

All four big brown bats performed similarly (both mean and individual performances are plotted in Fig. 3*B*). The bats perceived S+ echoes as having a discriminable delay even if only the lowest frequencies of 25 to 30 kHz in FM1 are present, but not vice versa. Progressively removing frequencies from 89 down to 34 kHz by low-pass filtering in small decrements visibly has no effect on the four bats' performance (mean percentage errors ±1 SD are shown as blue data points and curve; performance is well below the conventional 25% error threshold) until the low-pass cutoff falls from 34 to 29 kHz. Performance only deteriorates to rise above the threshold criterion of 25% errors when this low-frequency region is encroached upon (Fig. 3*B*). Finally, when all frequencies are removed from S+ by low-pass filtering at 20 kHz, there is no two-glint S+ at all, and the bats' performance reverts to near chance, indicating they search for the two glints but do not find them. High-pass filtering in the other direction reveals a different contingency. Progressively removing frequencies from 20 up to 68 kHz in small increments affects performance immediately (mean percentage errors ±1 SD are shown as red data points and curve). Filtering of echoes at 20 kHz preserves essentially the entire spectrum of the sounds, but filtering at 27 kHz causes performance to deteriorate to near 25% errors, and filtering at 31 kHz causes performance to decline beyond 25% errors. The collapse of discrimination occurs despite the unaffected presence of the majority of frequencies still in FM1 plus all of the frequencies in FM2 (spectrogram in Fig. 3*B*). This finding magnifies the previously discovered asymmetry of the two harmonics, FM1 and FM2 (Fig. 1*C*): The vast proportion of frequencies do not support perception of echo delay unless the critical frequencies of 25 to 30 kHz are present. That is, the discriminability of echo delay is anchored at the low-frequency end of FM1 (vertical orange arrow in Fig. 3*B*). Further evidence that these lowest frequencies are treated specially by big brown bats comes from prior experiments that exposed bats to jamming tones and monitored their performance in an echo detection task (35). The bat increases or decreases the terminal, tail end frequency of its FM1 sweep (i.e., frequency hopping) by up to 4 to 6 kHz in a classic jamming avoidance response to defend the reception of frequencies at 24 to 28 kHz (constant-frequency [CF] jamming, green triangles in Fig. 3*B*). The response is specific to these lowest frequencies; tonal jamming at other frequencies evokes no response from the bats.

Implications

From the low-pass and high-pass results, the critical frequencies of 25 to 30 kHz are both necessary and sufficient for big brown bats to perceive differences in echo delay. As a consequence of the downward direction of the FM sweeps in the bat's sounds (Fig. 1*A*), the essential 25 to 30 kHz lowest frequencies in FM1 are situated not only at the bottom of the broadcast spectrum in frequency but also at the end of the broadcast waveform in time. Echoes thus seem not to enter the bat's perception until the entire echo has been received and the required lowest frequencies are available to be processed for their delay. Evidently, echo processing begins at the lowest, tail end frequencies of FM1 and proceeds up the "ladder" of frequencies along the FM1 sweep, recruiting successively higher FM1 frequencies as well as the corresponding FM2 frequencies along the way (Fig. 1*C*). If the frequencies at the lowest rungs of the ladder are absent, no climbing along the FM sweeps is possible, and the echoes do not have discriminable delays. Failure of echoes to enter delay

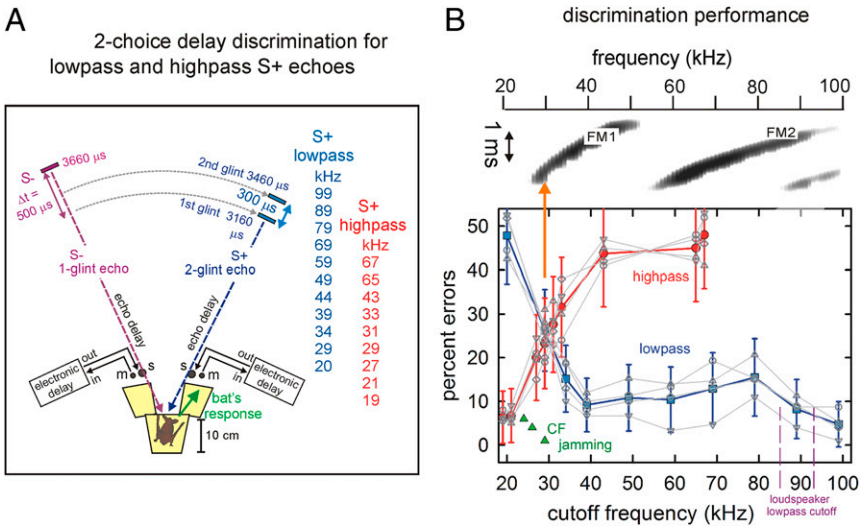

Fig. 3. Priority of lowest FM1 frequencies for delay perception. (*A*) Experiment to test whether the lowest FM1 frequencies of 25 to 35 kHz are both necessary and sufficient for echo delay discrimination. The bat on the Y-shaped platform is trained to broadcast sonar sounds into microphones (m, left and right) which lead to return of electronic "virtual reality" echoes from loudspeakers (s, also left and right). The correct response is to move forward toward the loudspeaker that delivers S+ echoes for a mealworm reward (rewarded S+, blue, 3,160 and 3,460 µs delays simulating distances of 54 and 60 cm and having easily perceived $\Delta t = 300$ µs glint separation versus unrewarded S–, purple, 3,660 µs delay, simulating 63 cm distance using a normally easily discriminated 500 µs longer delay than S+). Left–right positions of S+ and S– were randomized in experiments. Each stimulus condition (high-pass filtering, red list, or low-pass filtering, blue list) was tested for 150 trials per bat; performance was assessed as the percentage of correct responses (ranging from 0% perfect; to 50% chance). S+ echoes are subjected to sharp low-pass cutoff frequency (blue numbers) or high-pass cutoff frequency (red numbers) filtering (115 dB/octave cutoff frequencies in small steps from 99 down to 20 kHz or from 20 up to 68 kHz). (*B*) Two-choice results obtained for different high-pass and low-pass truncations of echo spectra. *Top* shows a spectrogram of a typical FM bat broadcast (frequency is horizontal, time is vertical; harmonics are FM1, FM2). *Bottom* shows the mean performance (±1 SD) of four big brown bats in two-choice tests with different high-pass (red) and low-pass (blue) cutoff frequencies. An individual bat's performance is shown in light gray. Error percentages show that the presence of frequencies around 29 to 32 kHz at the tail end of the FM1 sweep (orange vertical arrow) is essential; absent these frequencies, performance is near chance for all of the remaining frequencies, even if 70 to 80% of the other frequencies are still present (high-pass conditions). Additional confirmation that these frequencies are special comes from the results of previous jamming avoidance experiments (green triangles marking individual preferred frequencies and detection performance for three big brown bats; ref. 35). These bats defend a narrow span of frequencies (24 to 32 kHz) at the tail end of the FM1 sweep by shifting FM1 up or down, away from single-frequency jamming sounds at these frequencies. They do not react to jamming at other frequencies (35).

perception offers an elegant mechanism for the bat to segregate echo streams that differ in the low-frequency end of their spectra. The principal type of pulse-echo ambiguity occurs when long-delay echoes of the first broadcast intrude into the echo epoch for the second broadcast and are erroneously registered as short-delay echoes (Fig. 2*A* vs. Fig. 2*B*) (type II ambiguity, ref. 18). This ties into frequency hopping by big brown bats, which consists of increasing the low-frequency tail end of the FM sweep for the first of two closely spaced broadcasts relative to the second broadcast (Δf in Fig. 2*B*). Consequently, echoes of the first broadcast also terminate at slightly higher frequencies than echoes of the second broadcast (Fig. 2*B*). In light of the finding that the lowest FM1 frequencies are essential, echoes of the first broadcast lack the crucial low-frequency tail end of the FM1 sweeps that would be needed for them to be accepted as echoes of the second broadcast. Their absence means that they are not processed as echoes of the second broadcast, and the potential for ambiguity is prevented. Moreover, even though the frequency shifts ($\Delta f \sim 5$ to 7 kHz) observed in flying bats exposed to ambiguity are small relative to total echo bandwidth (75 to 80 kHz), they are large enough to cause a debilitating loss in delay acuity (Fig. 3*B*) in the perceptual scene reconstructed for the second broadcast. As a method for coping with pulse-echo ambiguity in wideband sonar, deliberately imposing poor delay acuity on the "wrong" echoes is an innovative approach, particularly as it takes place in the bat's perception, not just in preventing reception of the wrong echoes at an earlier stage of processing. In this sense it is related to recently identified mechanisms for rejecting clutter interference by blurring the perceived delay of clutter echoes relative to target echoes (40–42). The opposite case of ambiguity (type I ambiguity, ref. 18) occurs when echoes of the second broadcast, which have lower frequencies due to the direction of frequency hopping (Fig. 2) compared to the first broadcast, are misassigned to the first broadcast and registered as longer-delayed phantom objects. The absence of the lower frequencies prevents misassignment of echoes of the first broadcast relative to the second broadcast, but it does not prevent misassignment of echoes of the second broadcast to the first broadcast. Instead, these echoes differ in the shape of their FM sweeps from the first broadcast, and their ambiguity may be mitigated by the blurring effect as a kind of clutter (40–42).

The SCAT Receiver

Can the big brown bat's frequency-hopping solution be incorporated into a biologically inspired biosonar model that evades the limitations of conventional wideband processing with regard to pulse-echo ambiguity? Contemporary signal-processing methods employ digitally implemented transforms (e.g., Fourier transform) directly or indirectly to extract and display echo delay by the cross-correlation function of echoes with broadcasts (12, 30). Cross correlation is an optimally robust method for recognizing echoes that are even just marginally similar to broadcasts. From telemike recordings made during flight in an ambiguous situation (Fig. 2*B*) (16), spectrograms illustrate how similar big brown bat broadcasts and their echoes are even with frequency hopping (P1 and P2, E_{p1} and E_{p2}; Fig. 4*A*, close-up in Fig. 4*B*). The frequency shift (Δf) between the first and second broadcasts, which is mirrored in their echoes, does not obscure their overall

spectral overlap. The similarity of the ambiguous echo of P1 that follows P2 (E_{P1}) to echoes of P2 itself (E_{P2}) is shown quantitatively in Fig. 4*C* by the cross-correlation functions between P2 and the echoes that fall inside the echo epoch that follows it. The cross-correlation functions for both echoes of P2 (E_{P2}) have needlelike sharp peaks, indicating very accurate registration of their delay at the peaks, which is the optimal estimate for their delay, and only some slight spreading of the function around the peak (Fig. 4*C*) (30). The ambiguous echo, E_{P1}, which immediately follows P2, is mismatched to P2 in its lack of the lowest frequencies in the FM1 sweep of P2 (Fig. 4*B*). Nevertheless, it also has a strong cross-correlation function, with in this example a peak only about half the height of the cross-correlation functions for the two true echoes of P2 and a width only about twice that of the true, unambiguous echoes. The increased width registers the slight mismatch in the slope of the FM sweep for the ambiguous echo. The height of the cross-correlation function represents the total strength of the echo, which is slightly weakened by the mismatch. It might be thought that the lower cross-correlation peak would distinguish the ambiguous echo, E_{P1}, from real echoes of P2. The problem with this solution to ambiguity is that, in ordinary terms, each echo's strength represents the overall reflectivity of the target from its acoustic cross-section (12, 15, 30). In natural clutter such as vegetation, foliage surfaces comprising the scene fluctuate widely in reflective strength and distribution in depth, yielding masses of echoes that cannot be distinguished by echo strength or arrangement of glints (43–46). Consequently, an ambiguous echo of P1 does not reliably produce a weaker cross-correlation peak relative to P2 because correct echoes of P2 may themselves return echoes with lower cross-correlation peaks. That is, echo strength relative to the two broadcasts, and therefore cross-correlation peak height, acts, to some extent, as a stray parameter. Taken together, the three cross-correlation functions (Fig. 4*C*) indicate that the ambiguous echo E_{P1} is likely to be accepted as a slightly weaker putative echo of P2, just as the two true echoes E_{P2} are accepted as true echoes, albeit in this instance stronger. Upon acceptance, E_{P1} will be misrepresented as an echo of P2 and registered as a phantom object at close range, often, but not necessarily always, smaller than the true object. Even though the phantom object often appears slightly less reflective and slightly more dispersed in range than objects returning the true echoes E_{P2}, it is still part of the scene. This ambiguous outcome is exactly what frequency hopping is intended to prevent categorically.

In conventional transform-based receivers, all of the frequencies are extracted together; the transform has to run to completion before an estimate of echo delay appears on a purely time axis or its equivalent appears on a frequency axis (2, 30). However, a variety of other methods instead portray the FM signals on a two-dimensional time–frequency plane (47–49) instead of on a single time or frequency axis. Time–frequency methods have been applied to radar and sonar problems (50) and play a role in bioinspired receiver designs (13, 51). They have been used to examine echoes from targets used in experiments on echolocating dolphins or bats (52, 53). Time–frequency methods usually are based on transforms, too (e.g., short-term Fourier transform, Wigner–Ville transform; refs. 47–49). Applied to radar or sonar, they offer alternative computational routes to obtaining cross-correlation functions for pulses and echoes. The direct approach to time–frequency processing is to generate the frequency axis "up front," using a bank of band-pass filters at the moment signals are received. To mimic the inner ear's receptors, the spectrogram correlation and transformation (SCAT) model of biosonar (13) and its relatives (54–60) receive FM broadcasts and their echoes through parallel band-pass filters tuned to different frequencies in the bat's broadcast band. The current version of the SCAT method employs delay lines to determine target range and a multiresolution array of spectral filters that select different rates of spectral notches or ripples centered at different frequencies of the band-pass filter bank at the input (60) (https://github.com/gomingchen/SCAT). The outputs of these filters mark the time of occurrence of successive frequencies in the FM sweeps of broadcasts and echoes—an auditory version of a running spectrogram for the sounds reaching the bat's ears (compare Figs. 4*D* and 4*B*). Unlike cross correlation, the SCAT model estimates echo delay by comparing the response to the echo with the response to the preceding pulse separately in each frequency channel and then combining delay estimates across frequencies (the spectrogram correlation part of the model) (13, 54, 59). When implemented using bat-like FM signals and echoes, spectrogram correlation by itself is a triggered autocorrelation method (59) capable of performing similarly to cross correlation for estimating delay (61). Because delay is estimated in each frequency channel by marking the time of occurrence of each channel's response to the FM broadcast as time 0, followed by responses to the echoes at different delays as they are received, the initial display of delay aligns all of the responses to the broadcast at the same time 0 across channels (Fig. 4*E*). This "dechirps" the FM sweeps into vertically aligned time–frequency data points in broadcast P2 at zero time, removing the slope of the FM sweeps. The resulting display makes it easy to see how each echo's overall delay can be estimated by combining individual delay estimates vertically to make a histogram of their distribution across frequencies (red bars in Fig. 4*E*). This histogram is the SCAT model's version of the cross-correlation function for that echo (61). Note that the true echoes of P2 (E_{P2}) are represented very sharply (red histograms in Fig. 4*E*), just as they are sharply registered by the cross-correlation functions (Fig. 4*C*). The ambiguous echo (E_{P1}) is represented as more dispersed in time (red histogram in Fig. 4*E*), just as it is by the cross-correlation function (Fig. 4*C*). This dispersal reflects the slight mismatch in the slope of the FM sweeps for E_{P1} when it is compared to the dechirped broadcast P2. However, the ambiguous echo still is portrayed as a putative echo of P2 and a phantom object at close range.

Rejection of Ambiguous Echoes by the Modified SCAT Receiver

At this point, the implications of the psychophysical results (Fig. 3*B*) come into play: The bat initiates delay processing of each echo at the lowest frequencies in the broadcast and climbs upward along the FM sweep of the echo to build up its overall delay estimate. In the dechirped SCAT spectrograms (Fig. 4*E*), this is equivalent to building the overall delay histogram for each echo not just by equally pooling all of the delay estimates into the bar plot of their distribution but by beginning this "combining" at the lowest frequency in the broadcast and working up along the vertical row of time data points in successive filter channels. It requires only registering the low-frequency end of the most recent broadcast to start the process going. For the correctly matched echoes of broadcast P2 (E_{P2}), the lowest frequencies of about 21 to 22 kHz in the broadcast specify the frequencies at which delay processing is to begin. Because these echoes contain the same specified low frequencies, delay processing is initiated at the bottom of the vertical row of data points for each echo and moves up along the frequency axis, step by step, to finish the histogram (Fig. 4*F*). These echoes again are registered as having sharply defined delays (red histograms in Fig. 4*F*). However, the mismatched, intruding echo (E_{P1}) has its lowest, tail end frequencies around 26 to 27 kHz, not 21 to 22 kHz. In the absence of frequencies up to about 25 kHz from the dechirped data points at time 0 for P2, processing of the delay estimates for E_{P1} is not initiated. The higher frequencies are never drawn into the delay-estimating process that, otherwise, would lead to an ambiguous delay estimate for E_{P1} (Fig. 4*E*). In effect, the frequency ladder for the mismatched echo does not have its lowest

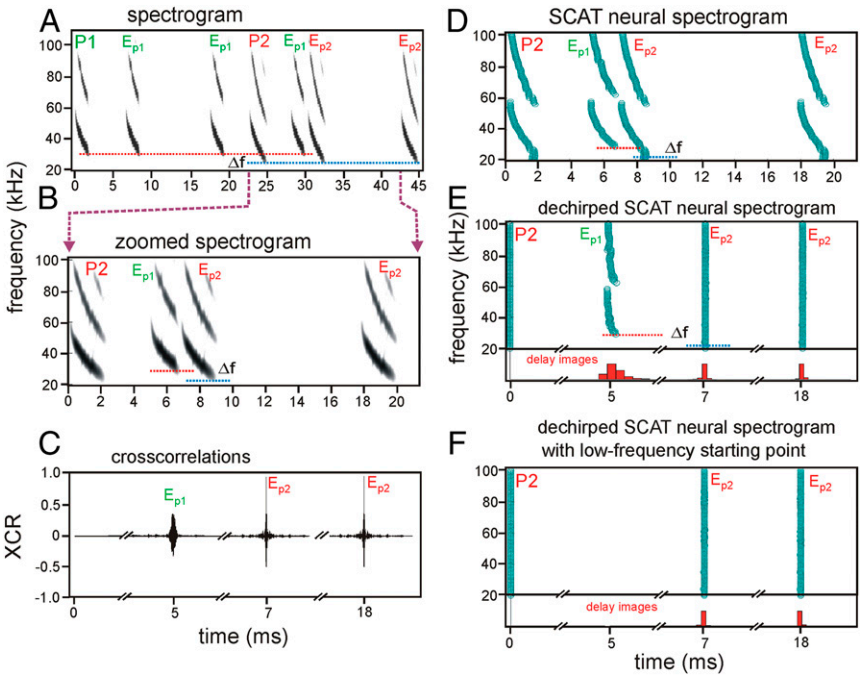

Fig. 4. The SCAT model can segregate echoes of different broadcasts by frequency hopping. (*A*) Spectrograms for two FM successive biosonar pulses with frequency hopping Δf (P1, P2) recorded using the telemike and several of their echoes (E_{P1}, E_{P2}) arranged in a sequence to test cross correlation (*B* and *C*) and SCAT determination of delay (*D*–*F*). (*B*) Spectrograms from *A* zoomed in to show P2 and the echoes that follow in its echo epoch. (*C*) Transformation of P2 and echoes from *B* into cross-correlation functions using P2 as the template. Both the correctly corresponding echoes (E_{p2}) and the ambiguous echo (E_{p1}) are highly correlated with P2, indicating acceptance of the ambiguous echo along with the correct echoes. Differences in cross-correlation peak height and cross-correlation width might seem adequate to reject the ambiguous echo, but height is the reflective object's size, and width is the object's shape, both of which vary considerably in real clutter such as vegetation (43–46), rendering them effectively stray parameters. (*D*) SCAT spectrograms for the same sounds as for the spectrograms in *B*. (*E*) SCAT can segregate echoes when the lowest frequencies are present. Dechirped spectrograms of signals in *D* plotted by shifting the time of occurrence of each frequency in P2 to time 0. Note vertical rows of points for both echoes E_{P2} and a slightly mismatched row of points for E_{P1}. (*F*) When the lowest frequencies in P2 are absent, SCAT cannot determine the delay estimate by frequency hopping.

rungs, so the onset of delay processing never happens, and no pulse-echo ambiguity occurs. Due to frequency hopping, the prevention of delay processing for mismatched echoes of an earlier broadcast (P1) with respect to the most recent broadcast (P2) does not just weaken the potentially ambiguous delay estimate (compare cross correlations in Fig. 4*C* or red histograms in Fig. 4*E*), it eliminates the ambiguous echo from perception entirely. This capability of the SCAT model shows the advantages of extracting the frequency axis of the spectrograms at the input to processing, when sounds are received, and incorporating the requirement that the lowest frequencies in the broadcast be present in the echo, too, for processing to occur. It allows the model to offer a wideband, technically implementable solution to pulse-echo ambiguity in dense, extended sonar or radar scenes, which is a significant goal for designing a novel biomimetic receiver (13).

Data Availability. All data and programs are accessible at GitHub, https://github.com/gomingchen/SCAT (62).

ACKNOWLEDGMENTS. We thank Andrea M. Simmons for extensive work editing the manuscript. This research was supported by grants from the Office of Naval Research N00014-14-1-05880 to J.A.S. and Office of Naval Research MURI N00014-17-1-2736 to J.A.S. and Andrea M. Simmons.

1. A. Kurta, R. H. Baker, Eptesicus fuscus. *Mamm. Species* **356**, 1–10 (1990).
2. D. R. Griffin, *Listening in the Dark*, (Yale University Press, New Haven, CT, 1958).
3. G. Neuweiler, *Biology of Bats*, (Oxford University Press, Oxford, UK, 2000).
4. M. B. Fenton, A. D. Grinnell, A. N. Popper, Eds., *Bat Bioacoustics*, (Springer, New York, 2016).
5. E. L. Clare, W. O. C. Symondson, M. B. Fenton, An inordinate fondness for beatles? Variation in seasonal dietary preferences of night-roosting big brown bats (*Eptesicus fuscus*). *Mol. Ecol.* **23**, 3633–3647 (2014).
6. J. A. Simmons, Big brown bats and June beetles: Multiple pursuit strategies in a seasonal acoustic predator-prey system. *Acoust. Res. Lett. Online* **6**, 238–242 (2005).
7. J. A. Simmons *et al.*, Delay accuracy in bat sonar is related to the reciprocal of normalized echo bandwidth, or *Q*. *Proc. Natl. Acad. Sci. U.S.A.* **101**, 3638–3643 (2004).
8. A. Surlykke, C. F. Moss, Echolocation behavior of big brown bats, *Eptesicus fuscus*, in the field and the laboratory. *J. Acoust. Soc. Am.* **108**, 2419–2429 (2000).
9. P. A. Saillant, J. A. Simmons, F. H. Bouffard, D. N. Lee, S. P. Dear, Biosonar signals impinging on the target during interception by big brown bats, Eptesicus fuscus. *J. Acoust. Soc. Am.* **121**, 3001–3010 (2007).
10. C. F. Moss, A. Surlykke, Probing the natural scene by echolocation in bats. *Front. Behav. Neurosci.* **4**, 33 (2010).
11. C. F. Moss, K. Bohn, H. Gilkenson, A. Surlykke, Active listening for spatial orientation in a complex auditory scene. *PLoS Biol.* **4**, e79 (2006).
12. M. I. Skolnik, *Introduction to Radar Systems*, (McGraw-Hill, New York, ed. 2, 1980).
13. P. A. Saillant, J. A. Simmons, S. P. Dear, T. A. McMullen, A computational model of echo processing and acoustic imaging in frequency-modulated echolocating bats: The spectrogram correlation and transformation receiver. *J. Acoust. Soc. Am.* **94**, 2691–2712 (1993).
14. J. A. Simmons, The resolution of target range by echolocating bats. *J. Acoust. Soc. Am.* **54**, 157–173 (1973).
15. W. P. Stilz, H. U. Schnitzler, Estimation of the acoustic range of bat echolocation for extended targets. *J. Acoust. Soc. Am.* **132**, 1765–1775 (2012).
16. S. Hiryu, M. E. Bates, J. A. Simmons, H. Riquimaroux, FM echolocating bats shift frequencies to avoid broadcast-echo ambiguity in clutter. *Proc. Natl. Acad. Sci. U.S.A.* **107**, 7048–7053 (2010).
17. A. R. Wheeler *et al.*, Echolocating big brown bats, *Eptesicus fuscus*, modulate pulse intervals to overcome range ambiguity in cluttered surroundings. *Front. Behav. Neurosci.* **10**, 125 (2016).
18. M. L. Melcón, Y. Yovel, A. Denzinger, H.-U. Schnitzler, How greater mouse-eared bats deal with ambiguous echoic scenes. *J. Comp. Physiol. A Neuroethol. Sens. Neural Behav. Physiol.* **197**, 505–514 (2011).

19. J. R. Barchi, J. M. Knowles, J. A. Simmons, Spatial memory and stereotypy of flight paths by big brown bats in cluttered surroundings. *J. Exp. Biol.* **216**, 1053–1063 (2013).
20. C. Chiu, W. Xian, C. F. Moss, Adaptive echolocation behavior in bats for the analysis of auditory scenes. *J. Exp. Biol.* **212**, 1392–1404 (2009).
21. B. Falk, L. Jakobsen, A. Surlykke, C. F. Moss, Bats coordinate sonar and flight behavior as they forage in open and cluttered environments. *J. Exp. Biol.* **217**, 4356–4364 (2014).
22. J. M. Knowles, J. R. Barchi, J. E. Gaudette, J. A. Simmons, Effective biosonar echo-to-clutter rejection ratio in a complex dynamic scene. *J. Acoust. Soc. Am.* **138**, 1090–1101 (2015).
23. N. B. Kothari, M. J. Wohlgemuth, K. Hulgard, A. Surlykke, C. F. Moss, Timing matters: Sonar call groups facilitate target localization in bats. *Front. Physiol.* **5**, 168 (2014).
24. A. E. Petrites, O. S. Eng, D. S. Mowlds, J. A. Simmons, C. M. DeLong, Interpulse interval modulation by echolocating big brown bats (*Eptesicus fuscus*) in different densities of obstacle clutter. *J. Comp. Physiol. A Neuroethol. Sens. Neural Behav. Physiol.* **195**, 603–617 (2009).
25. S. Sändig, H.-U. Schnitzler, A. Denzinger, Echolocation behaviour of the big brown bat (Eptesicus fuscus) in an obstacle avoidance task of increasing difficulty. *J. Exp. Biol.* **217**, 2876–2884 (2014).
26. J. A. Simmons, S. Hiryu, U. Shriram, Biosonar interpulse intervals and pulse-echo ambiguity in four species of echolocating bats. *J. Exp. Biol.* **222**, jeb195446 (2019).
27. H. K. Markley, G. Antheil, "Secret communication system." US Patent 2292387 (1942).
28. A. Guillén-Servent, C. Ibáñez, Unusual echolocation behavior in a small molossid bat, *Molossops temminckii,* that forages near background clutter. *Behav. Ecol. Sociobiol.* **61**, 1599–1613 (2007).
29. E. C. Mora, S. Macías, M. Vater, F. Coro, M. Kössl, Specializations for aerial hawking in the echolocation system of *Molossus molossus* (Molossidae, Chiroptera). *J. Comp. Physiol. A Neuroethol. Sens. Neural Behav. Physiol.* **190**, 561–574 (2004).
30. P. M. Woodward, *Probability and Information Theory with Applications to Radar*, (Pergamon Press, New York, ed. 2, 1953).
31. C. F. Moss, H.-U. Schnitzler, Accuracy of target ranging in echolocating bats: Acoustic information processing. *J. Comp. Physiol. A Neuroethol. Sens. Neural Behav. Physiol.* **165**, 383–393 (1989).
32. S. A. Stamper, M. E. Bates, D. Benedicto, J. A. Simmons, Role of broadcast harmonics in echo delay perception by big brown bats. *J. Comp. Physiol. A Neuroethol. Sens. Neural Behav. Physiol.* **195**, 79–89 (2009).
33. M. E. Bates, J. A. Simmons, Effects of filtering of harmonics from biosonar echoes on delay acuity by big brown bats (*Eptesicus fuscus*). *J. Acoust. Soc. Am.* **128**, 936–946 (2010).
34. J. A. Simmons, M. Ferragamo, C. F. Moss, S. B. Stevenson, R. A. Altes, Discrimination of jittered sonar echoes by the echolocating bat, *Eptesicus fuscus*: The shape of target images in echolocation. *J. Comp. Physiol. A Neuroethol. Sens. Neural Behav. Physiol.* **167**, 589–616 (1990).
35. M. E. Bates, S. A. Stamper, J. A. Simmons, Jamming avoidance response of big brown bats in target detection. *J. Exp. Biol*. **211**, 106–113 (2008).
36. J. A. Simmons, Convergence of temporal and spectral information in target images perceived by the echolocating bat, *Eptesicus fuscus*. *J. Comp. Physiol. A Neuroethol. Sens. Neural Behav. Physiol.* **166**, 449–470 (1990).
37. C. F. Moss, H. U. Schnitzler, "Behavioral studies of auditory information processing" in *Hearing by Bats*, A. N. Popper, R. R. Fay, Eds. (Springer Handbook of Auditory Research, Springer, New York, 1995), pp. 87–145.
38. U. Shriram, J. A. Simmons, Echolocating bats perceive natural-size targets as a unitary class using micro-spectral ripples in echoes. *Behav. Neurosci.* **133**, 297–304 (2019).
39. W. W. L. Au, J. A. Simmons, Echolocation in dolphins and bats. *Phys. Today* **60**, 40–45 (2007).
40. M. E. Bates, J. A. Simmons, T. V. Zorikov, Bats exploit echo harmonic structure to distinguish targets from clutter and suppress interference. *Science* **333**, 627–630 (2011).
41. J. A. Simmons, Bats use a neuronally implemented computational acoustic model to form sonar images. *Curr. Opin. Neurobiol.* **22**, 311–319 (2012).
42. J. A. Simmons, Temporal binding of neural responses for focused attention in biosonar. *J. Exp. Biol.* **217**, 2834–2843 (2014).
43. R. Müller, R. Kuc, Foliage echoes: A probe into the ecological acoustics of bat echolocation. *J. Acoust. Soc. Am.* **108**, 836–845 (2000).
44. Y. Yovel, M. O. Franz, P. Stilz, H. U. Schnitzler, Plant classification from bat-like echolocation signals. *PLOS Comput. Biol.* **4**, e1000032 (2008).
45. C. Ming, A. K. Gupta, R. Lu, H. Zhu, R. Müller, A computational model for biosonar echoes from foliage. *PLoS One* **12**, e0182824 (2017).
46. C. Ming, H. Zhu, R. Müller, A simplified model of biosonar echoes from foliage and the properties of natural foliages. *PLoS One* **12**, e0189824 (2017).
47. L. Cohen, *Time-Frequency Analysis*, (Prentice Hall, New York, 1995).
48. A. Mertens, A. Mertens, *Signal Analysis: Wavelets, Filter Banks, Time-Frequency Transforms and Applications*, (Wiley, New York, 1999).
49. B. Boashash, *Time Frequency Signal Analysis and Processing*, (Elsevier, New York, ed. 2, 2016), pp. 577–625.
50. G. C. Gaunaurd, H. C. Strifors, Signal analysis by means of time-frequency (Wigner-type) distributions-applications to sonar and radar echoes. *Proc. IEEE* **84**, 1231–1248 (1996).
51. A. Balleri, H. Griffiths, A. Stove, C. Baker, Eds., *Biologically Inspired Radar and Sonar: Lessons from Nature*, (IET Press, London, 2017).
52. G. C. Gaunaurd, D. Brill, H. Huang, P. W. B. Moore, H. C. Strifors, Signal processing of the echo signatures returned by submerged shells insonified by dolphin "clicks:" Active classification. *J. Acoust. Soc. Am.* **103**, 1547–1557 (1998).
53. C. M. Delong, R. Bragg, J. A. Simmons, Evidence for spatial representation of object shape by echolocating bats (Eptesicus fuscus). *J. Acoust. Soc. Am.* **123**, 4582–4598 (2008).
54. H. Peremans, J. Hallam, The spectrogram correlation and transformation receiver, revisited. *J. Acoust. Soc. Am.* **104**, 1101–1110 (1998).
55. I. Matsuo, K. Kunugiyama, M. Yano, An echolocation model for range discrimination of multiple closely spaced objects: Transformation of spectrogram into the reflected intensity distribution. *J. Acoust. Soc. Am.* **115**, 920–928 (2004).
56. M. Park, R. Allen, Pattern-matching analysis of fine echo delays by the spectrogram correlation and transformation receiver. *J. Acoust. Soc. Am.* **128**, 1490–1500 (2010).
57. K. Georgiev, A. Balleri, A. Stove, M. W. Holderied, Bio-inspired processing of radar target echoes. *Radar Sonar Navigation IET* **12**, 1402–1409 (2018).
58. J. A. Simmons, J. A. Gaudette, M. Warnecke, "Biosonar inspired signal processing and acoustic imaging from echolocating bats" in *Biologically Inspired Radar and Sonar: Lessons from Nature*, A. Ballieri, H. Griffiths, A. Stove, C. Baker, Eds. (IET Press, London, 2017), pp. 5–34.
59. L. Wiegrebe, An autocorrelation model of bat sonar. *Biol. Cybern.* **98**, 587–595 (2008).
60. N. Neretti, N. I. Sanderson, N. Intrator, J. A. Simmons, Time-frequency computational model for echo-delay resolution in sonar images of the big brown bat, *Eptesicus fuscus*. *J. Acoust. Soc. Am.* **113**, 2137–2145 (2003).
61. M. I. Sanderson, N. Neretti, N. Intrator, J. A. Simmons, Evaluation of an auditory model for echo delay accuracy in wideband biosonar. *J. Acoust. Soc. Am.* **114**, 1648–1659 (2003).
62. C. Ming, SCAT model. GitHub. https://github.com/gomingchen/SCAT. Deposited 15 June 2020.